

ARTIFICIAL NEURAL NETWORK MODELLING OF THE TENSILE PROPERTIES OF INDIGENOUSLY DEVELOPED 15Cr-15Ni-2.2Mo-Ti MODIFIED AUSTENITIC STAINLESS STEEL

**P.V. Sivaprasad, Sumantra Mandal, Sridhar Venugopal,
C. Narayanan, V. Shanmugam and Baldev Raj**

Metallurgy and Materials Group
Indira Gandhi Centre for Atomic Research,
Kalpakkam-603102, Tamil Nadu, India
E-mail : prasad@igcar.gov.in

(Received 24 April 2006 ; in revised form 16 May 2006)

ABSTRACT

The severe and hostile operating conditions of fast breeder reactors demand the development of new austenitic stainless steels that possess higher resistance to void swelling and irradiation embrittlement. This paper discusses the efforts made in the laboratory and industrial scale development of a 15Cr-15Ni-2.2Mo-Ti modified austenitic stainless steel and the evaluation of tensile properties. Melting and casting were carried out in a vacuum induction furnace and the data on recovery of various alloying elements was obtained for charge calculations. Based on the recovery data and decarburisation behaviour under different vacuum levels, a series of alloys with close chemistry variations were prepared. Heat treatment was optimised for these special steels to control the grain size at required level. The ingots were thermo-mechanically processed and tensile properties were evaluated. This experimental data has been used to train and test an artificial neural network. The input parameters of the neural network are chemical compositions and test temperature while the yield strength, ultimate tensile strength and uniform elongation were obtained as output. A multilayer perceptron (MLP) based feed-forward network with back-propagation learning algorithm has been employed. A very good performance of the developed network is obtained. The model can be used as a guideline for new alloy development.

1. INTRODUCTION

The selection of materials for clad and wrapper depends on the design criteria. For the Fast Breeder Reactor project (PFBR) of Indian nuclear programme, the design criteria included operating temperatures in the range of 673-973 K and 673-873 K for clad and wrapper respectively, under steady state operating conditions. Under transient conditions, the temperatures can rise upto 1273 K and 1073 K for clad and wrapper respectively. Major loads on the fuel clad are the internal pressure due to accumulated fission gases released from fuel matrix (~ 5 MPa) and moderate fuel-clad interaction. Major loads on the hexcan are the internal pressure due to sodium

coolant (~ 0.6 MPa) and the interaction loads at the contact pads due to bowing of the subassemblies under temperature and swelling gradients. Slight thermal stresses due to transients are also present because of the higher thickness of the wrapper. The main mechanical properties that govern the choice of clad and wrapper materials are tensile properties in the case of wrapper, and both tensile and creep properties in the case of clad. Besides high temperatures and stresses, materials in fast reactor core are also subjected to very demanding environment of high fast neutron flux ($\sim 10^{15}$ n cm⁻² s⁻¹). One major consequence of the high flux of fast neutrons is the occurrence of very high levels of radiation damage in the core structural materials.

The main factor that currently limits fast reactor fuel life, and thus the burn-up, is void swelling. The void swelling produces dimensional changes in the wrapper and thus makes the loading and unloading operations difficult. Therefore the main challenge in fast reactors materials technology today is the development of low swelling materials for in-core applications. Austenitic stainless steels have been chosen worldwide as materials for in-core applications owing to their excellent elevated temperature mechanical properties, compatibility with liquid sodium and adequate resistance to void swelling¹. AISI type 316 and its modifications have been used as materials for fuel subassemblies seeing a dose of ≈ 65 dpa (displacements per atom). However, a commercial fast breeder power reactor would demand development of materials with improved swelling resistance at damage levels greater than 125 dpa.

In order to meet the requirements for the core components of PFBR, a programme was undertaken for the indigenous development of alloy D9 (15Cr-15Ni-2.2Mo-Ti modified austenitic stainless steel). The paper discusses the indigenous development of alloy D9, optimisation of melting, casting, forging and solution annealing treatments. Further, an attempt is made to correlate the tensile properties to chemical composition. Basically there are two ways to understand such correlations. Firstly, one can construct a physical model that describe the relation between parameters, and subsequently validate this model with experimental findings^{2,3}. However an explicit physical model that quantitatively describes all the correlations between alloy composition, processing parameters and tensile properties of austenitic stainless steel does not exist. Alternatively, a model can be developed applying statistical techniques⁴ like multi-linear regression methods. However, in austenitic stainless steel, the effects of alloying elements on mechanical properties are complex and the synergistic interactions of the effects of individual alloying elements play a major role than the influence of individual element. Another limitation of multi-linear regression is the time required to evaluate the constants is high and its accuracy of prediction is low.

In this perspective, artificial neural network (ANN) can be considered as an efficient modeling tool. Though artificial neural network modeling is a relatively new technique, in past few years there has

been a rapidly increasing interest in neural network modeling in different fields of material science⁵⁻⁸. In essence, ANN is an advanced statistical technique that links input to output data using a particular set of non-linear functions and has the potential to solve problems that can not be efficiently solved by other conventional statistical models such as regression analysis⁹. The basic advantage of employing ANN approach lies in the fact that they do not require any external manifestation of parametric relationships. An ANN learns from examples and recognizes patterns in a series of input and output values without any prior assumptions about their nature and interrelations. Therefore, it can automatically and efficiently map the complicated inter-relationships between various parameters¹⁰. Provision of model free solutions, data error tolerance and built in dynamism makes the network attractive. Therefore, an ANN model has been developed for the prediction of tensile properties of alloy D9 as a function of alloy composition and test temperature.

2. EXPERIMENTAL

Alloys of different compositions with varying carbon levels in the range 0.026-0.13 and Ti/C ratios in the range 3 – 8 were prepared in Balzer's VSG30 vacuum induction melting (VIM) and casting unit. A vacuum level of 10^{-5} torr was maintained during melting. The laboratory ingots were subjected to non-destructive evaluation of defects using X-ray radiography and ultrasonic testing to identify and locate casting defects. The ingots were and then cold swaged to 11 mm diameter rounds for mechanical property evaluation in solution annealed as well as cold worked condition. Metallographic investigation of the material in the as-cast, hot-forged and the final solution annealed conditions were carried out to characterize the material. Tensile tests were carried out on 20% cold worked samples in a universal testing machine, at a strain rate of $3.14 \times 10^{-4} \text{ s}^{-1}$ at room temperature as well as at 923 K. Button head type specimens of 26 mm gauge length and 4 mm gauge diameter were employed for tensile testing. The load-elongation data was analyzed for evaluating tensile properties such as yield stress, ultimate tensile stress and uniform elongation using standard equations.

The melting and processing variables for commercial production were optimized based on the experience

obtained on laboratory heats. Commercial scale melting of three heats with Ti/C ratios of 4, 6 and 8 have been made at MIDHANI, Hyderabad, from virgin raw materials through VIM with ladle adjustment to achieve desired Ti/C ratio. This was followed by vacuum arc remelting. Rounds of 30 mm diameter were produced through hot forging and hot rolling. These rounds were reduced to 11 mm diameter by cold swaging. Tensile tests were carried out on 20% cold worked samples for this commercial scale melting. Studies on the recrystallization behaviour and microstructural stability under different ageing conditions have also been carried out on samples cold worked to different levels. Commercial alloy rods of 30 mm diameter were annealed at 1343K for 30 minutes and then cold worked from 2.5% to 30% in a universal testing machine. Specimens were cut from these cold worked rods and hardness measurements were carried out.

3. RESULTS AND DISCUSSION

The melting trials established that selection of the right quality of raw materials and close control of melting parameters are important to ensure elimination of oxidation and nitridation of alloying elements and resultant non-metallic inclusions. So, the raw materials used for melting were analyzed for both desirable and trace elements. The chemistry of the alloys produced in the laboratory was controlled effectively by charge calculations, taking into account the decarburization and vaporization losses of alloying elements as a function of melt hold time. Standardization of charge calculations and melting parameters were achieved after extensive experimental studies on melting under different conditions. The percentage recovery of various alloying elements, particularly C, Mn, Ti, were computed based on the experimental heats and found to be ~80%. On the other hand, the recovery of Cr, Mo and Ni were found to be higher than 95%. This recovery data has been employed for initial charge calculations to obtain various alloys with the required chemical composition. The following melting procedures were found to be effective in controlling the chemistry of the different alloys melted in 5 and 10 kg batches using magnesia crucibles and cast iron moulds:

i. Initial evacuation of the melting chamber to high vacuum levels (10^{-5} torr).

- ii. Reducing the melting down time to thirty minutes, by avoiding bridging using suitable charge placement.
- iii. Adding C, Mn and Ti towards the end of the melting operation.
- iv. Careful control of melt temperature to avoid high vaporization losses and improve both life of crucible and mould.
- v. Pouring the melt in a thin stream under high vacuum to ensure effective degassing.
- vi. Selection of raw materials for alloy additions in the elemental form. (This was found to be more reliable because of the macro inhomogeneities in the composition of the ferro-alloys in different lumps).

Non-destructive testing of the ingots revealed a small amount of centre line porosity and a few shrinkage cavities. The ingots were sectioned along these defects and shaped before hot working. One hundred percent visual inspection was found necessary during all the intermediate stages of forming like hot forging and hot rolling, since lower working temperatures resulted in cracking. Homogenization treatment of the ingots at 1323 K for two hours produced best results during hot forging. The optimum conditions for achieving the required grain size were obtained on the basis of vacuum annealing experiments and grain size measurement and a typical heat treatment cycle is illustrated in Fig.1. All the cold swaged rods and the cold rolled sheets were annealed, following this procedure to achieve a uniform optimum grain size in all the test specimens, in a programmable vacuum furnace.

The nuclear specification demands that the inclusion content determined as per ASTM E-45 should conform to the following:

- (a) 1 for thin and $\frac{1}{2}$ for heavy for individual type A,B,C,D
- (b) Total of A,B,C and D (thin + heavy) 4

Inclusion counting was carried out on the laboratory-melted samples in both longitudinal and transverse sections of the (a) as-cast, (b) cast and forged and (c) cast, forged and rolled materials. In the case of cast

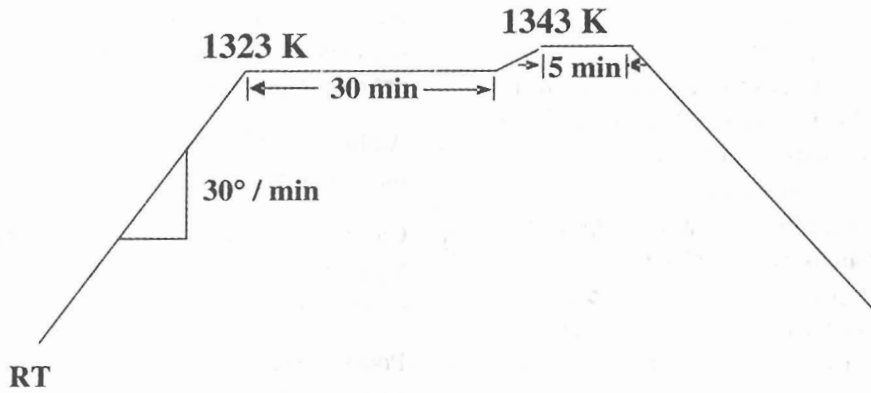


Fig. 1: Heat treatment schedule for achieving the required grain size and microstructure

material, samples were taken from top, middle and bottom portion of the ingot. In all the samples, the inclusions were found to be mostly of oxide type in the thin series range. The inclusion rating of these samples varied from 2 to 4 in the ingot stage which got refined with hot working. On the other hand, in the commercial samples, A, B and C type inclusions were absent and only D type inclusions with a value of 0.5 were observed. This improvement achieved through double melting/refining in commercial production.

Production of cold worked microstructures stable at service temperatures is one of the important metallurgical variables controlling void swelling, other than the composition of the alloy. It is also shown that stability of microstructure on elevated temperature irradiation could be related to stability on thermal exposure. Fig.2 shows the effect of cold work on hardness. The hardness at different cold-worked and ageing conditions is shown in Fig.3. During this study some interesting microstructural features were observed and these are shown in Fig.4. Cuboidal TiCN second phases are seen in these alloys under all conditions. The annealed samples exhibit bimodal grain size distribution at a certain combination of cold worked and ageing conditions, where incipient recrystallization starts.

The value of yield strength of the commercially melted alloy D9 at various test temperature is shown in Fig.5(a). It can be seen that yield strength value of the 20% cold worked sample with Ti/C of 6 are well within the acceptable limits of PFBR specifications. Similar trend has also been obtained

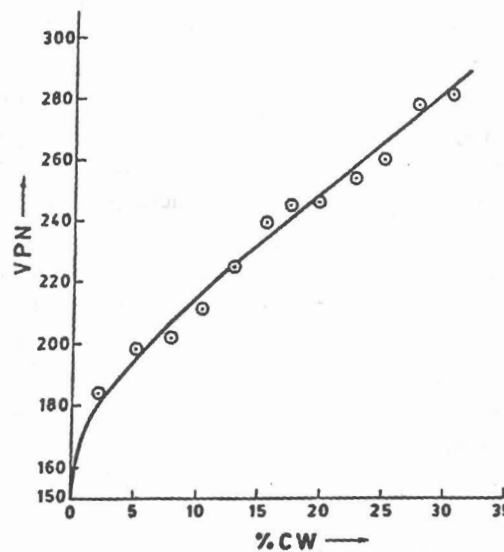


Fig. 2: The effect of cold worked on the hardness of commercial heat with Ti/C ratio 4.

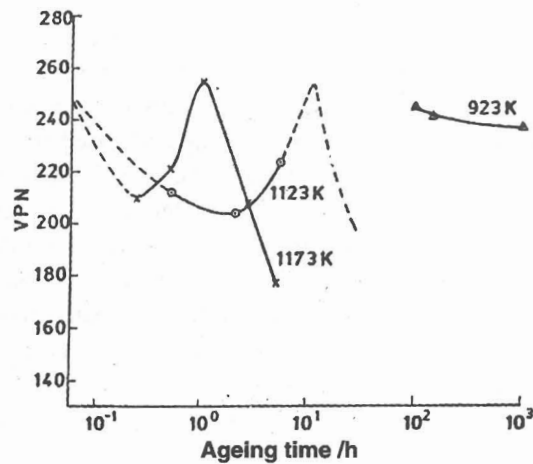


Fig. 3: Recrystallization kinetics of 20% cold worked commercial with Ti/C ratio 4

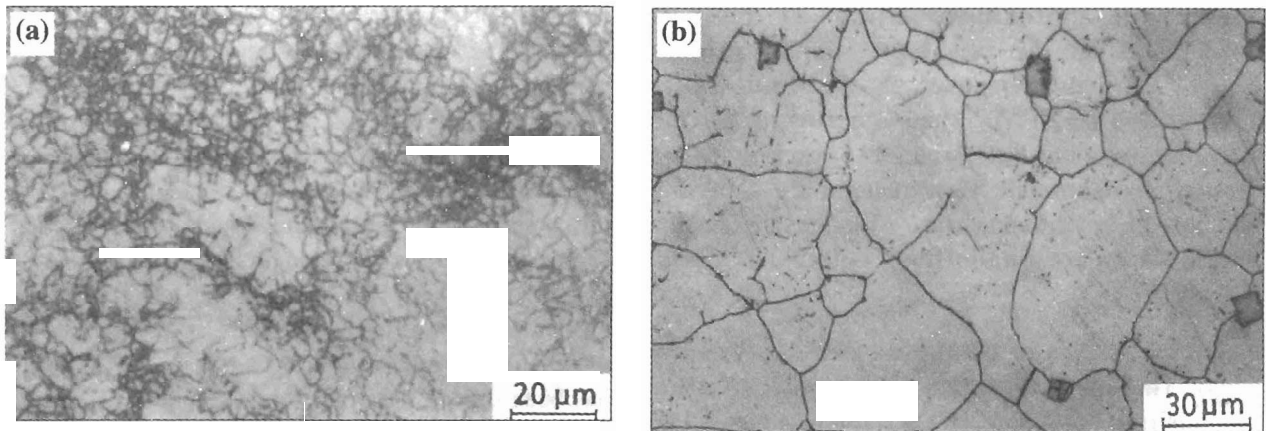


Fig. 4: Optical micrograph of cold worked alloy D9 aged at 1073K for 2 hour. The cold worked levels are (a) 5% (b) 10%

for ultimate tensile strength and uniform elongation and thereby not shown here. The complex dependence of strength with respect to the Ti/C ratio in these alloys can be seen in Fig.5(b) where properties of the annealed conditions are shown. One can discern a reversal of trend in the strength as function of the Ti/C ratio. This could be due to the fact that dependence of strength is related to the amount of carbon present in solution. However, fine TiC precipitates, when present could also lead to strengthening. This would be balanced against the decrease in strength due to loss of carbon in solution. The yield strength vs. test temperature plot shows a hump in the solution annealed condition (Fig.5b) and a plateau in the cold worked condition (Fig.5a). This behaviour is attributed to dynamic strain ageing.

Further, the associated embrittlement observed in this temperature regime is also reflected in the ductility values.

3.1 ANN Model overview

In this study, a multilayer perceptron (MLP) based feed-forward network has been trained by standard back propagation (BP) learning algorithm. MLP based network is used since it has greater representational power for dealing with highly non-linear, strongly coupled and multivariable system ¹¹. Although multilayer neural network does not ensure a global minimum solution for any given problem, it is a reasonable approximation that if the network is trained with a comprehensive database, the resulting

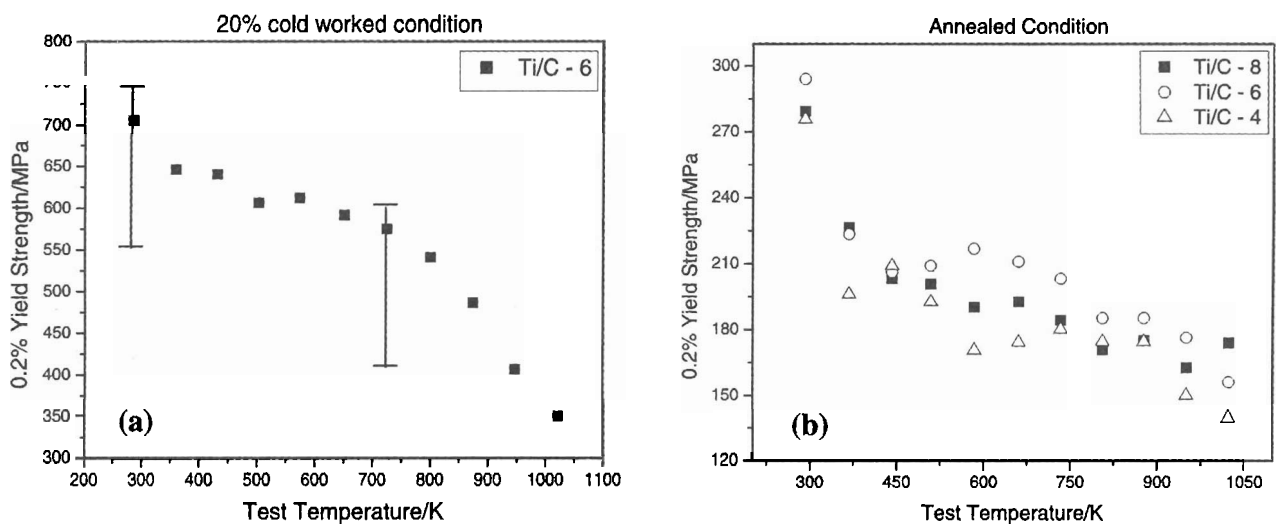


Fig. 5: Temperature dependence of yield strength of alloy D9 in (a) 20% cold worked and (b) solution annealed condition

model will approximate all of the laws of mechanics that the actual material or process obeys¹². A logistic sigmoidal function expressed as $Output = (1 + e^{-input})^{-1}$ was employed as the activation function; the learning is based on gradient descent algorithm and hence requires the activation function to be differentiable. More details on the neural network modelling could be found elsewhere^{13,14}.

A general scheme of the present model is given in Fig.6. The input parameters of the model are alloy composition and test (work) temperature. The compositions included are the five important alloying elements in alloy D9: C, Ni, Mn, Cr and Mo. Other alloying elements and grain size are not considered since they don't have significant variation in the data set. Omitting the parameter which is almost constant in data set benefits the development of the model and simplifies further application¹⁵. Test temperature is

included since this material will be used in the elevated temperature (the design criteria of this material includes operating temperatures in the range of 673-973K and 673-873K for clad and wrapper respectively, under steady state operating conditions). The outputs of the neural network are the three important tensile properties namely yield strength (YS), ultimate tensile strength (UTS) and uniform elongation (UE). The database obtained from the tensile tests of the lab melt ingot has been employed to develop the model. Out of this database, 75% data has been used for training while remaining 25% has been employed for testing. The statistical features of the input compositions and outputs are depicted in Table 1 and Table 2 respectively.

3.2 Model performance

The ANN model with one hidden layer has been found sufficient for this study. This observation

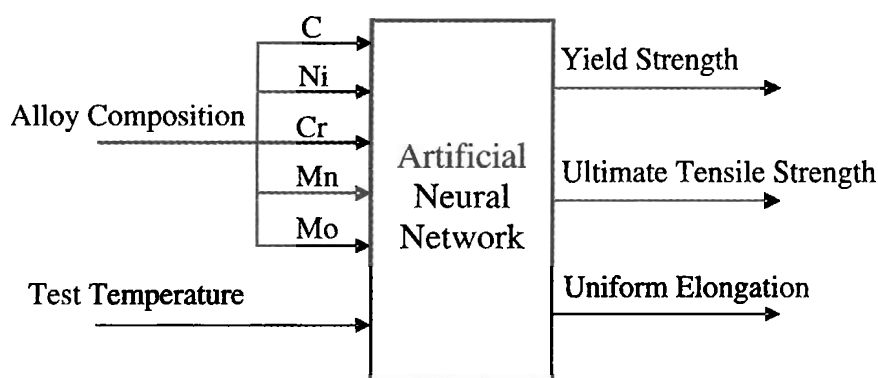


Fig. 6: Schematic model of the artificial neural network for prediction of tensile properties in alloy D9

Table 1
STATISTICAL ANALYSIS OF THE INPUT COMPOSITIONS

Inputs (wt%)	Maximum	Minimum	Std. Dev ⁿ	Mean
C	0.13	0.026	0.02592	0.06597
Ni	15.9	14.64	0.27152	15.2242
Cr	15.92	15.0	0.18737	15.5661
Mn	2.73	0.94	0.45177	1.8353
Mo	2.41	2.06	0.06241	2.1704

Table 2
STATISTICAL ANALYSIS OF THE OUTPUT DATA

Outputs	Maximum	Minimum	Std. Dev ⁿ	Mean
YS (MPa)	805.4	307.4	129.67	598.4
UTS (MPa)	859.4	420.9	143.35	636.0
UE (%)	23.0	3.71	6.41	11.2

reaffirms the universal approximation theorem that a single layer of non-linear hidden units is sufficient to approximate any continuous function. Hornik et al. ¹⁶ have also shown that a three layer ANN with sigmoid transfer function can map any function of practical interest. We determined the optimal number of neurons in the hidden layer by comparing the performance of the network, with 1-20 hidden neurons, and choose the number that produced the greatest network performance. For example, the performance of the network for yield strength prediction at different hidden unit level is shown in Fig.7. From the plot it is easily understood that optimum training with minimum average root mean square (RMS) training and test error is obtained when number of hidden neurons is 14 (shown by arrow in Fig.7). So, ANN with one hidden layer and 14 hidden neurons is the optimum model for yield strength prediction.

The performance of the model for yield strength (YS) prediction has been demonstrated in Fig.8. The figure indicates the network reliability in form of

linear regression analysis between the networks outputs i.e. predicted data and the corresponding experimental findings. It could be observed that a very good agreement exists between the experimental and predicted data. Almost similar performance has been obtained from the model for ultimate tensile strength (UTS) prediction.

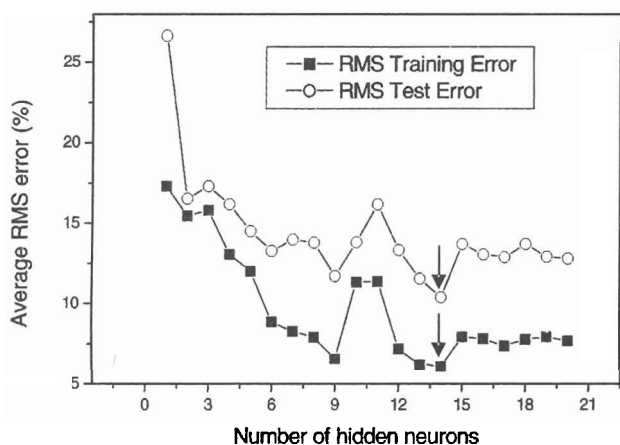


Fig. 7: RMS error as a function of number of hidden neuron for yield strength (YS) prediction

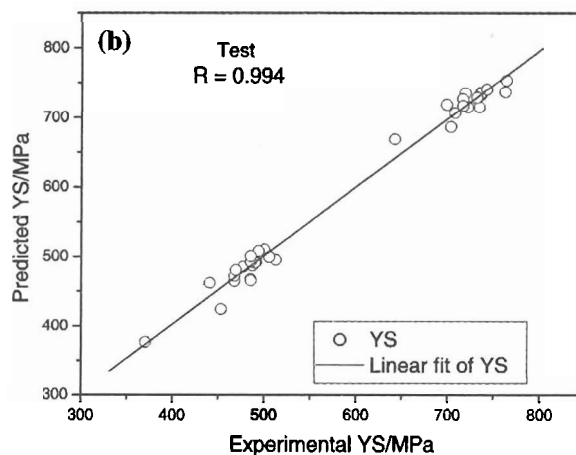
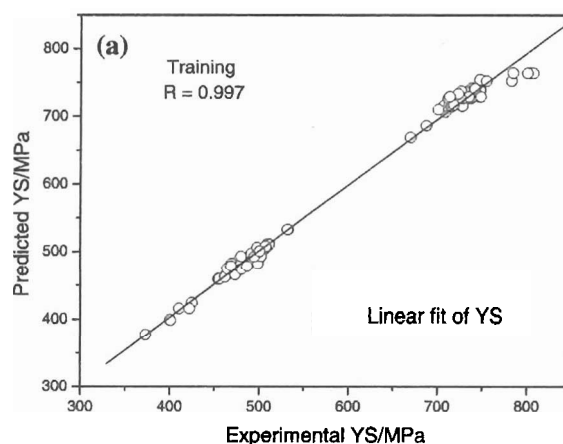


Fig. 8: Performance of the neural network model for prediction of yield strength (YS), plotting the experimental vs. predicted data points for the (a) training and (b) test

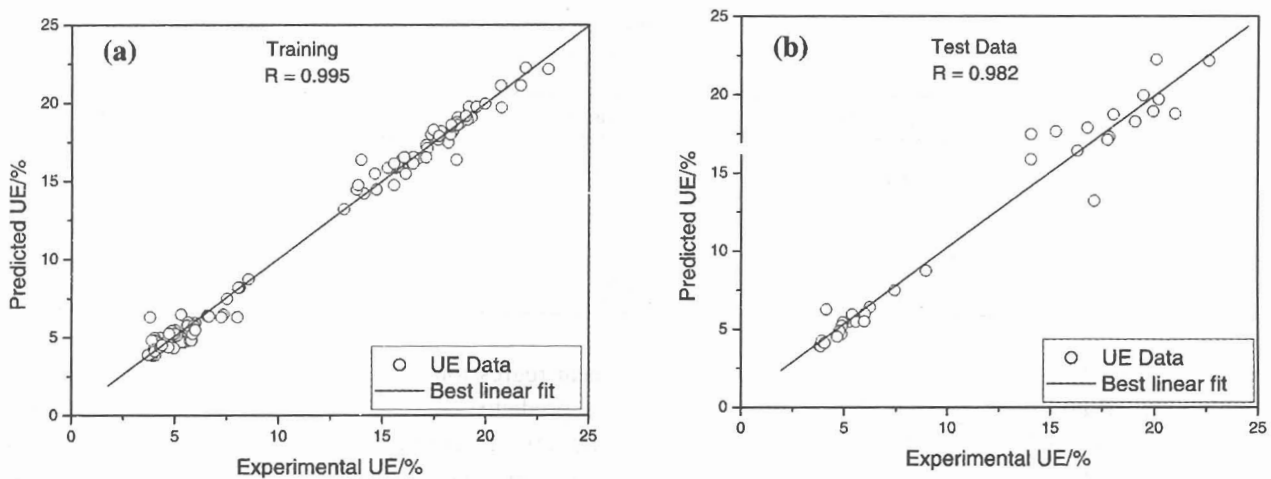


Fig. 9: Performance of the neural network for prediction of uniform elongation (UE) for the (a) training and (b) test data set

The quality of the model for uniform elongation (UE) prediction on different datasets is demonstrated in Fig.9. The prediction accuracy for UE is fairly good. However, the level of accuracy for UE is not as good as that of YS or UTS. The reason can be attributed to the sensitivity of ductility related parameter to experimental factors. Ductility related parameters like uniform elongation are more easily influenced by experimental factors, such as specimen condition and dimension, than strength parameters like yield strength or ultimate tensile strength. To investigate how sensitive the output parameters of the developed ANN are to fluctuations (noise) in the input data, the following Monte Carlo sensitivity analysis was carried out. We select arbitrary nominal values of the six input parameters from the training range: $\hat{C} = 0.062$; $\hat{Ni} = 15.16$; $\hat{Cr} = 15.79$; $\hat{Mn} = 1.93$; $\hat{Mo} = 2.11$ and $\hat{T} = 923K$. We assume C, Ni, Cr, Mn, Mo and T to be Gaussian random variables with mean equal to \hat{C} , \hat{Ni} ,

\hat{Cr} , \hat{Mn} , \hat{Mo} and \hat{T} with 5% relative standard deviation (noise). The logic behind this assumption lies in the fact that the relative error of ANN predictions has been found to follow Gaussian distribution. C, Ni, Cr, Mn, Mo and T is sampled independently and randomly from their respective distribution and fed as inputs to the ANN which returns yield strength (YS), ultimate tensile strength (UTS) and uniform elongation (UE) as output. This exercise was carried out 1000 times. It has been observed that due to this 5% fluctuation (noise) in the input variables, the corresponding fluctuations in YS and UTS are mere 7.48% and 6.25% respectively. However, a significant fluctuation (~25%) is observed for UE which reiterates the fact that ductility related parameters like UE are much more sensitive to input noise as compared to strength related parameters like YS or UTS. Similar exercise was carried out with 1% fluctuations in the input parameters. In this time also, the fluctuations in YS

Table 3
SUMMARY OF THE RESULTS FOR EACH TENSILE PROPERTY MODEL

Tensile Property	Average RMS Error	Correlation Coefficient (R)	Number of hidden neurons
YS	Training: 6.07 Test: 10.38	Training: 0.997 Test: 0.994	14
UTS	Training: 6.68 Test: 8.14	Training: 0.997 Test: 0.997	12
UE	Training: 0.44 Test: 0.82	Training: 0.995 Test: 0.982	7

and UTS are only 2.5% and 1.88% respectively while UE shows a substantial fluctuations of ~10%. This analysis, therefore, suggest that lower accuracy level for UE prediction could not be attributed to the predictive capability of ANN. Rather it should be ascribed to the noise in the experimental data arises due to inevitable fluctuations in alloy compositions along with the unavoidable variations in experimental factors, such as specimen condition and dimension.

The summary of the model for each tensile property is given in Table 3.

4. CONCLUSION

The following conclusions are drawn from the present study:

- i) A 15Cr-15Ni-2.2Mo-Ti modified austenitic stainless steel (alloy D9) has been indigenously developed in laboratory. The melting and casting procedure is standardised. Based on the recovery data of various alloying elements, industrial scale alloys were prepared.
- ii) Tensile properties were evaluated for both the lab and commercial heats. The tensile properties of the commercially melted ingot were found to be well within the acceptable limits of PFBR specifications.
- iii) The database obtained from the tensile testing of the laboratory heats were employed to develop an artificial neural network model to correlate alloy composition and test temperature to tensile properties.
- iv) It has been demonstrated that the developed network is capable of predicting tensile properties of alloy D9 with sufficient accuracy. The model can be used as a guideline for development of new austenitic stainless steels with the required tensile properties.

REFERENCES

1. Mannan S L, and Sivaprasad P V, *Encyclopedia of Materials Science and Technology*, (eds.) K.H.Jurgen Buschow, Robert W Cahn, Merton C Flemings, Bernhard Ilshner, Edward J Kramer and Subash Mahajan, Elsevier, New York (2001), p 2857.
2. Shereliff H R, and Ashby M F, *Acta Metal Mater* **38** (1990) 1789.
3. Guo Z, Sha W, and Wilson E A, *Mater Sci Technol* **18** (2002) 377.
4. Ganguly R I, and Dhindaw B K, *Met Technol* (April) (1978) 114
5. Badmos A Y, Bhadeshia H K D H, and Mackay D J C, *Mater Sci Technol*, **14** (1998) 793
6. Venkatesh V, and Rack H J, *Inter J Fatigue*, **21** (1999) 225
7. Calcaterra S, Campana G, and Tomesani L, *J Mater Process Technol*, 104 (2000) 74
8. Mandal S, Sivaprasad P V, and Dube R K, *J mater Sci*, (in press)
9. McBride J, Malinov S, and Sha W, *Mater Sci Eng A*, **384** (2004) 129
10. Rao H S, Mukherjee A, *Computational Mater Sci*, **5** (1996) 307
11. Juang S C, Tarang Y S, and Lii H R, *J Mater Process Technol*, **75** (1998) 54
12. Chuan M S, Biglou J, Lenard J G, and Kim J G, *J Mater Process Technol*, **86** (1999) 245
13. Haykin S, *Neural Networks: A Comprehensive Foundation*, Prentice Hall, New Jersey, (1999).
14. Guessasma S, and Coddet C, *Acta Mater*, **52** (2004) 5157
15. Guo Z, and Sha W, *Computational Mater Sci*, **29** (2004) 12
16. Hornik K, Stinchcombe M, and White H, *Neural Networks*, **2** (1989) 359.